Journal of Sound and Vibration (2000) **229**(2), 287–310
Article No. jsvi.1999.2490, available online at http://www.idealibrary.com on IDEAL®

NON-LINEAR DYNAMICS OF GEAR-PAIR SYSTEMS WITH PERIODIC STIFFNESS AND BACKLASH

S. THEODOSSIADES AND S. NATSIAVAS

Department of Mechanical Engineering, Aristotle University, 54006 *Thessaloniki, Greece*

(*Received* 27 *July* 1998, *and in final form* 11 *June* 1999)

The present work investigates dynamics of a gear-pair system involving backlash and time-dependent mesh stiffness. In addition, the system is under the action of external excitation, caused by torsional moments and gear geometry errors. First, the equation of motion is established in a strongly non-linear form. Then, the emphasis is laid on a specific forcing frequency range, corresponding to conditions of simultaneous fundamental parametric resonance and principal external resonance. For these conditions, several types of periodic steady state response are identified and determined by employing suitable methodologies, including techniques applicable to piecewise linear systems and to oscillators with time-periodic coefficients. Moreover, these methodologies are complemented by appropriate procedures revealing the stability properties of the located periodic solutions. In the second part of the work, numerical results are presented. These results verify the validity and effectiveness of the new analytical methodology and provide information on the gear-pair dynamics. First, series of typical response diagrams are obtained, illustrating the effect of the mesh stiffness variation, the damping and the forcing parameters on the gear-pair periodic response. These response diagrams are accompanied by results obtained with direct integration of the equation of motion. In this way, it is demonstrated that for some parameter combinations, the dynamical system examined can exhibit more complicated and irregular response, including crises and intermittent chaos.

1. INTRODUCTION

Gear mechanisms have found extensive application in modern power transmission systems, due to their considerable technical advantages. In many cases, the special geometrical characteristics of the gear teeth affect the dynamics and vibrational behavior of geared systems in a significant way. As a consequence, research in the area of dynamics of mechanical systems involving gear mechanisms has been intensive, especially over the past 40 years (see, e.g., references [1–4] and references therein). These previous studies focused on developing involved models of geared systems and analyzed torsional vibration, coupling of lateral-torsional vibration, gyroscopic and foundation effects as well as the influence of transmission errors. However, in the presence of gear backlash, which is either introduced intentionally at the design stages or caused by manufacturing errors and wear, the equations of motion of such systems become strongly non-linear. Another important

0022-460X/00/020287 + 24 $35.00/0

complication arises from the variable number of gear teeth pairs which are in contact at a time, causing a variation of the equivalent gear meshing stiffness. These two factors introduce serious difficulties in the analysis and obscure the interpretation of the numerical results.

Recently, the interest towards developing a better understanding of gear vibration has been renewed. This interest is reflected clearly in some new studies, which have dealt with relatively simple models of geared mechanical systems (see e.g., references [5–9]). The main effort of all these studies was to throw more light on fundamental issues related to the interaction of non-linear effects such as gear backlash and support non-linearities with time-periodic variations of the gear meshing stiffness. The important dynamics associated with this interaction is captured by models expressed by piecewise linear or non-linear equations of motion with time-periodic coefficients and external forcing. In particular, this forcing is generated by either torsional moments or by errors in gear geometry. Typically, the determination of the vibrational response of these models was performed either by direct integration [6] or by applying other common numerical methodologies, like the trigonometric collocation, the harmonic balance and the shooting method [5, 7, 8].

The main objective of the present study is to apply a new analytical methodology for determining periodic steady state motions, together with their stability properties, for simple gear-pair systems. Similar methods, suitable for piecewise linear systems with time-periodic coefficients, were originally presented in reference [10]. Here, this analysis is first extended by considering more general external forcing conditions and more solution types of a gear-pair system. More specifically, the emphasis is laid on analyzing the response of gear-pairs for the special but practically most important case of simultaneous fundamental parametric resonance and principal external resonance. First, the results are presented in the form of response diagrams and provide information on the system dynamics. This information is also useful in evaluating the validity of some simpler gear-pair models, which are frequently employed in practice. Moreover, the information obtained from the stability analysis is used in identifying parameter ranges where the gear-pair system examined possesses and exhibits complicated vibrational response.

The validity and effectiveness of the new methodology is established by direct comparison with results obtained from direct integration. Also, the main steps of the analysis are presented in a way that permits extension of the method to other forcing conditions in a straightforward manner. In addition, the same methodology can easily be employed in capturing periodic motions of many other categories of mechanical systems with similar dynamic characteristics (see, e.g., references [11, 12]).

The organization of the present paper is as follows. First, the mechanical model and the corresponding equation of motion, which captures the essential dynamic response of a typical gear-pair system, are briefly presented in the following section. In section 3 periodic response to simultaneous fundamental parametric resonance and principal external resonance is analyzed. Several types of periodic steady state motions are first defined and then determined, by applying analytical methodologies which are appropriate for piecewise linear systems with

time-periodic coefficients. These methodologies are then complemented by suitable techniques, determining the stability properties of the located periodic motions. In section 5, some special but extensively employed gear-pair models are examined. Finally, numerical results are presented in section 6. Initially, the influence of the meshing stiffness variation, the damping and the external forcing parameters on the periodic motions is illustrated by a series of response diagrams. Next, direct integration is performed, revealing the presence of some other types of response, including subharmonic and chaotic motions. In the final section, a summary of the work is presented.

2. MECHANICAL MODEL

The mechanical model of the gear-pair system investigated in the present study is shown in Figure 1. According to this two-degree-of-freedom torsional model, the centers of both gears are not allowed to move laterally. In addition, the total rotation angle of each gear is assumed to result from a constant angular velocity term plus a small variation due to vibrations originating from the flexibility of the mating gear teeth. This means that

$$\varphi_n(t) = \omega_n t + \theta_n(t) \quad (n = 1, 2)$$

where ω_1 and ω_2 are the constant angular velocity components of the gears. Moreover, the stiffness of the model depends on the number and position of the gear teeth pairs which are in contact and is a periodic function of the relative angular position of the gears. The model takes into account the so-called static

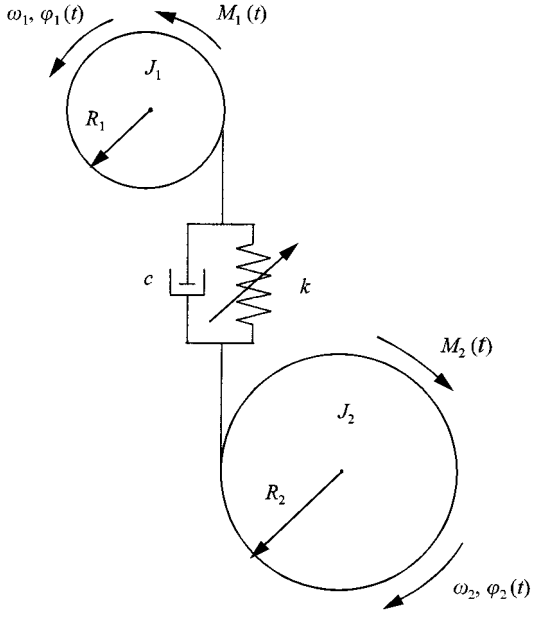

Figure 1. Mechanical model.

transmission error, which represents geometrical errors of the teeth profile and spacing. Since the mean angular velocities of the gears are constant, both the stiffness and the static transmission error quantities can approximately be considered as time-periodic functions. In addition, if the tooth to tooth variations (i.e., pitch errors and runout of teeth) are neglected, the fundamental frequency of both of these quantities equals the gear meshing frequency

$$\omega_M = n_1\omega_1 = n_2\omega_2,$$

where the integers n_1 and n_2 stand for the teeth number of each gear. This implies that the meshing stiffness and the static transmission error terms can be expressed in a Fourier series form. For instance, the model stiffness can be expressed in the form

$$k(t) = k_0 + \sum_{s=1}^{\infty} [\, p_s \cos(s\omega_M t) + q_s \sin(s\omega_M t)].$$

For the mechanical model examined, the equations of motion are first set up with respect to the two torsional co-ordinates $\varphi_1(t)$ and $\varphi_2(t)$. Then employing the composite co-ordinate

$$x(t) = R_1\varphi_1(t) - R_2\varphi_2(t) - e(t),$$

where R_1 and R_2 represent the base radii of the gears, results in elimination of the rigid-body rotation of the original model and yields a single equation of motion in the form

$$m\ddot{x} + c\dot{x} + k(t)h(x) = f_T(t) + f_M(t) \tag{1}$$

with

$$m = \frac{J_1J_2}{J_1R_2^2 + J_2R_1^2}, \quad f_T(t) = \frac{R_1J_2M_1(t) - R_2J_1M_2(t)}{J_1R_2^2 + J_2R_1^2}, \quad f_M(t) = -m\ddot{e}(t)$$

where J_1 and J_2 are the mass moments of inertia of the gears. Moreover, the forcing term $f_T(t)$ includes the contribution of the external torque loads $M_1(t)$ and $M_2(t)$ applied on the system and the excitation term $f_M(t)$ arises from the gear static transmission error, while

$$h(x) = \begin{cases} x - b, & x \geqslant b, \\ 0, & |x| < b, \\ x + b, & x \leqslant -b, \end{cases}$$

where $2b$ represents the total backlash. Next, introducing the parameters

$$\omega_0 = \sqrt{\frac{k_0}{m}}, \quad \zeta = \frac{c}{2\sqrt{mk_0}}, \quad \Omega_M = \frac{\omega_M}{\omega_0}, \quad \hat{t} = \omega_0 t, \quad w(\hat{t}) = \frac{k(t)}{k_0}, \quad u(\hat{t}) = \frac{x(t)}{b}$$

the original equation of motion (1) can eventually be put in the normalized form

$$\ddot{u} + 2\zeta\dot{u} + w(t)g(u) = f(t), \tag{2}$$

In the last equation, the symbol $\hat{t}$ has been replaced by t for simplicity, while the stiffness coefficient is a periodic function of time, i.e., $w(t + T_M) = w(t)$ with

fundamental period $T_M = 2\pi/\Omega_M$ and constant term equal to unity. Moreover, the function $g(u)$ is expressed as

$$g(u) = \begin{cases} u - 1, & u \geqslant 1, \\ 0, & |u| < 1, \\ u + 1, & u \leqslant -1, \end{cases}$$

while the term $f(t)$ includes forcing effects due to external torques as well as due to geometric irregularities of the mating gear teeth.

3. PERIODIC RESPONSE

The dynamical model expressed by the equation of motion (2) has been employed in previous research work [6–8]. Its validity has also been investigated by comparison with experimental results [6, 7]. Among other types of response, this equation is expected to accept periodic steady state solutions. However, the process of determining these solutions analytically presents two serious difficulties. The first one is caused by the presence of backlash, which renders this equation strongly non-linear. The second complication arises from the presence of the time-periodic mesh stiffness terms. As a consequence, there appears to exist no systematic analytical methodology leading to exact solutions of equation (2). This implies that only approximate solutions of this equation can be obtained at best.

Due to the aforementioned difficulties, it turns out that in any attempt to capture periodic solutions of the equation of motion (2), the frequency ranges of interest should be specified from the outset. Therefore, among all the possible cases, the present study focuses on revealing the important dynamics of the gear-pair system within a frequency range presenting large practical interest. Namely, if Ω represents the gear meshing frequency Ω_M (or a multiple of it), the frequency range examined is chosen according to the condition

$$\Omega = 1 + \varepsilon\sigma, \tag{3}$$

where ε is a small positive number. In this case, it is expected that the following special form of the original equation of motion

$$\ddot{u} + 2\varepsilon\mu\dot{u} + (1 + 2\varepsilon\cos\Omega t)g(u) = f_0 + \varepsilon f_1\cos(\Omega t + \theta), \tag{4}$$

will provide sufficiently accurate results. For this system, approximate periodic solutions can be obtained by generalizing and applying a method presented in reference [10]. This method combines characteristics of the approaches employed for piecewise linear systems involving constant coefficients (see, e.g., references [13–18]) with classical perturbation techniques applied to dynamical systems involving time-varying coefficients [19]. More specifically, several possible types of periodic steady state solutions of the equation of motion (4) are first identified. Then, for small values of the parameter ε, the characteristics of each of these solutions are determined by applying standard perturbation techniques and by imposing appropriate sets of periodicity and matching conditions.

3.1. TYPE I PERIODIC MOTIONS

For some combinations of the system parameters and for particular choices of the starting conditions, the gear-pair oscillations remain always within the $u \geqslant 1$ range. This is classified as a type I motion and involves no impacts of the mating gears. In this case, the gear-pair dynamics is governed by the linear equation of motion

$$\ddot{u} + 2\varepsilon\mu\dot{u} + (1 + 2\varepsilon\cos\Omega t)(u - 1) = f_0 + \varepsilon f_1 \cos(\Omega t + \theta). \tag{5}$$

Then, for sufficiently small values of the parameter ε, application of the multiple time-scales method [19] furnishes approximate solutions of equation (5) in the asymptotic series form

$$u(t) = u_0(\tau_0, \tau_1, \tau_2) + \varepsilon u_1(\tau_0, \tau_1, \tau_2) + \varepsilon^2 u_2(\tau_0, \tau_1, \tau_2) + O(\varepsilon^3),$$

with $\tau_n = \varepsilon^n t$. More specifically, by substituting this series form into equation (5), performing the algebra and separating the terms with different order of ε yields the following system of equations:

$$D_0^2 u_0 + u_0 = 1 + f_0,$$

$$D_0^2 u_1 + u_1 = -2D_0 D_1 u_0 - 2\mu D_0 u_0 - 2(u_0 - 1)\cos\Omega t + f_1 \cos(\Omega t + \theta),$$

$$D_0^2 u_2 + u_2 = -2D_0 D_1 u_1 - (D_1^2 + 2D_0 D_2)u_0 - 2\mu(D_0 u_1 + D_1 u_0) - 2u_1 \cos\Omega t,$$

with $D_n \equiv \partial/\partial\tau_n$. Then, following standard perturbation approaches [19] and performing lengthy algebraic manipulations, the solution of the last set of linear equations is determined in the form

$$u_0 = 1 + f_0 + a\cos(\Omega t - \gamma), \quad u_1 = -a\cos\gamma + \tfrac{1}{3}a\cos(2\Omega t - \gamma)$$

and

$$u_2 = -\tfrac{4}{9}a\sigma\cos(2\Omega t - \gamma) + \tfrac{1}{24}a\cos(3\Omega t - \gamma) - \tfrac{4}{9}f_0\cos 2\Omega t + \tfrac{2}{9}f_1\cos(2\Omega t + \theta),$$

respectively, where the unknown amplitude a and the phase γ satisfy a set of autonomous equations

$$\dot{a} = -\varepsilon\mu a - c_1\sin\gamma - c_2\cos\gamma + c_3\sin(\gamma + \theta) + c_4\cos(\gamma + \theta) + \tfrac{1}{2}\varepsilon^2 a\sin 2\gamma, \tag{6}$$

$$a\dot{\gamma} = c_5 a + c_2\sin\gamma - c_1\cos\gamma - c_4\sin(\gamma + \theta) + c_3\cos(\gamma + \theta) + \tfrac{1}{2}\varepsilon^2 a\cos 2\gamma, \tag{7}$$

with coefficients

$$c_1 = (\varepsilon - \tfrac{1}{2}\varepsilon^2\sigma)f_0,\ c_2 = \tfrac{1}{2}\mu\varepsilon^2 f_0,\ c_3 = (\tfrac{1}{2} - \tfrac{1}{4}\sigma\varepsilon)\varepsilon f_1,\ c_4 = \tfrac{1}{4}\mu\varepsilon^2 f_1,$$

$$c_5 = \varepsilon\sigma + (\tfrac{1}{3} + \tfrac{1}{2}\mu^2)\varepsilon^2.$$

Therefore, the approximate solutions of equation (5) within the frequency ranges specified by equation (3) take the form

$$u(t) = 1 + f_0 + a\cos(\Omega t - \gamma) - \varepsilon a[\cos\gamma - \tfrac{1}{3}\cos(2\Omega t - \gamma)] - \varepsilon^2[\tfrac{4}{9}a\sigma\cos(2\Omega t - \gamma)$$
$$- \tfrac{1}{24}a\cos(3\Omega t - \gamma) + \tfrac{4}{9}f_0\cos 2\Omega t - \tfrac{2}{9}f_1\cos(2\Omega t + \theta)] + O(\varepsilon^3). \tag{8}$$

As can be concluded from the last expression, constant solutions of the slow-flow set of equations (6) and (7) correspond to periodic motions of the mechanical oscillator, with fundamental frequency Ω. Such solutions can be determined analytically. By imposing the conditions $\dot{a} = \dot{\gamma} = 0$, the resulting system of algebraic equations can be put in the form

$$a \sin 2\gamma = e_1 a + e_2 \sin\gamma + e_3 \cos\gamma, \quad a \cos 2\gamma = e_4 a + e_5 \sin\gamma + e_6 \cos\gamma. \tag{9}$$

Proper elimination of the trigonometric terms from the last set of equations leads to a fourth order polynomial in a^2. This polynomial can be solved in closed form for the vibration amplitude a. Subsequently, the corresponding phase γ can be determined by simple back-substitution.

3.2. TYPE II PERIODIC MOTIONS

When the steady state response assumes maximum values greater than 1 and minimum values below 1 but above -1, it is characterized as a type II motion and involves single-sided impacts of the gear-pair. Taking into account the information depicted in Figure 2(a), the equation of motion within the time interval $0 \leqslant t_1 \leqslant t_{1c}$ is first expressed in the form

$$\ddot{u}_1 + 2\varepsilon\mu\dot{u}_1 + [1 + 2\varepsilon\cos(\Omega t_1 + \varphi)](u_1 - 1) = f_0 + \varepsilon f_1 \cos(\Omega t_1 + \theta + \varphi). \tag{10}$$

Here, the constant phase φ is introduced into both the parametric and the external forcing terms in order to assure that the initial displacement equals one. In addition, for small values of the parameter ε, approximate solutions of equation (10) are sought in the regular perturbation series form

$$u_1(t_1) = u_{01}(t_1) + \varepsilon u_{11}(t_1) + \varepsilon^2 u_{21}(t_1) + O(\varepsilon^3). \tag{11}$$

As usual, the main problems associated with a regular perturbation series are caused by the so-called secular and the small divisor terms they produce when substituted into the original equation of motion [19]. However, since the time interval examined here ($0 \leqslant t_1 \leqslant t_{1c}$) is finite and relatively small, it is anticipated that there is not enough time for secular terms of this series expansion to grow and cause problems, as was the case in reference [10] and verified by numerical results in section 6. Moreover, small divisor terms can properly be eliminated, by making use of the frequency condition (3). Therefore, substituting equation (11) into equation (10) and collecting terms proportional to ε^0, ε^1 and ε^2 yields a set of linear equations, whose solution furnishes eventually the solution of equation (10) in the form

$$u_1(t_1) = A_1 a_1(t_1; \varphi) + B_1 b_1(t_1; \varphi) + c_1(t_1; \varphi). \tag{12}$$

The functions $a_1(t_1; \varphi)$, $b_1(t_1; \varphi)$ and $c_1(t_1; \varphi)$ are obtained after a quite involved algebraic manipulation in terms of the system parameters and the phase φ.

Next, the response within the time interval $0 \leqslant t_2 \leqslant t_{2c}$ is determined by considering the corresponding form of the equation of motion, which now becomes

$$\ddot{u}_2 + 2\zeta\dot{u}_2 = f_0 + \hat{f_1} \cos(\Omega t_2 + \theta + \varphi)$$

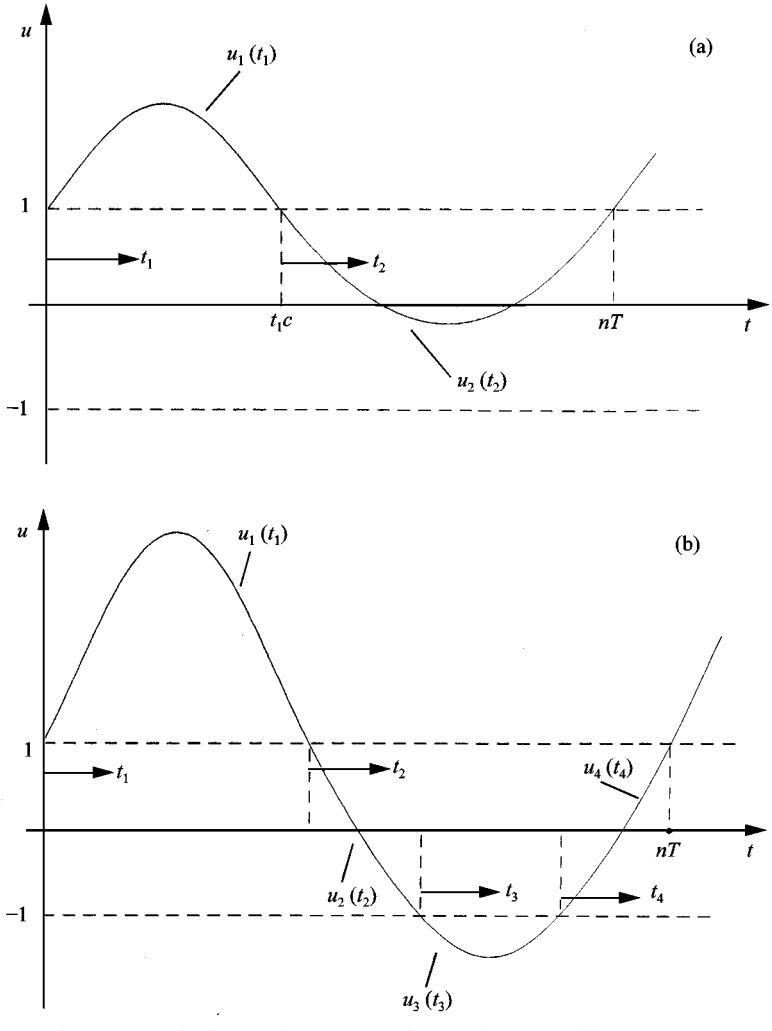

Figure 2. Periodic steady state motions: (a) type II; (b) type III.

with $\hat{f}_1 = \varepsilon f_1$. The last equation accepts the following exact solution.

$$u_2(t_2) = A_2 e^{-2\zeta t_2} + B_2 + C_2 t_2 + D_2 \cos(\Omega t_2 + \theta + \varphi - \psi) \tag{13}$$

with

$$C_2 = \frac{f_0}{2\zeta}, \quad D_2 = \frac{\hat{f}_1}{\Omega\sqrt{\Omega^2 + 4\zeta^2}}, \quad \cos\psi = \frac{-\Omega}{\sqrt{\Omega^2 + 4\zeta^2}}, \quad \sin\psi = \frac{2\zeta}{\sqrt{\Omega^2 + 4\zeta^2}}. \tag{14}$$

Based on the above formulation, the determination of type II periodic motions has been reduced to the evaluation of the constants A_1, B_1, A_2, B_2, φ and the crossing time t_{1c}. These constants can be determined by applying the following set of periodicity and matching conditions:

$$u_1(0) = u_1(t_{1c}) = u_2(0) = u_2(t_{2c}) = 1, \tag{15–18}$$

$$\dot{u}_1(0) = \dot{u}_2(t_{2c}) \equiv \dot{u}_{10}, \quad \dot{u}_1(t_{1c}) = \dot{u}_2(0) \equiv \dot{u}_{20} \tag{19, 20}$$

where $t_{2c} = nT - t_{1c}$, n is an integer and $T = 2\pi/\Omega$. The solution of the resulting set of six transcendental equations is simplified by first applying the displacement conditions (17) and (18). This leads to a linear system for A_2 and B_2 with form

$$\begin{bmatrix} 1 & 1 \\ e^{-2\zeta t_{2c}} & 1 \end{bmatrix} \begin{pmatrix} A_2 \\ B_2 \end{pmatrix} = \begin{pmatrix} 1 - D_2 \cos(\theta + \varphi - \psi) \\ 1 - C_2 t_{2c} - D_2 \cos(\Omega t_{2c} + \theta + \varphi - \psi) \end{pmatrix}.$$

A similar but more complicated set of equations is then obtained for A_1 and B_1 by applying the conditions (15) and (16). In both systems, the coefficients depend on the system parameters, the phase φ and t_{1c} only. Therefore, solving the last two systems of equations for A_1, B_1, A_2 and B_2 and substituting the resulting expressions into the velocity conditions (19) and (20) generates a system of two algebraic equations for the phase φ and the crossing time t_{1c} only. Numerical solution of these equations determines φ and t_{1c}, by taking into account that their values lie inside the intervals $(0, 2\pi)$ and $(0, nT)$, respectively. Then, the corresponding values of A_1, B_1, A_2 and B_2 are determined by simple backsubstitution, while the corresponding type II periodic solution is obtained from equations (12) and (13).

3.3. TYPE III PERIODIC MOTIONS

When a periodic motion of equation (3) exhibits a maximum displacement value larger than 1 and a minimum value smaller than -1, the gear-pair motion involves double-sided impacts and is characterized as a type III motion (Figure 2(b)). Application of a methodology similar to that presented for the type II motions shows that the determination of this new solution type requires the solution of a set of 12 transcendental equations. This set results by imposing the following system of periodicity and matching conditions:

$$u_1(0) = u_1(t_{1c}) = u_2(0) = u_4(t_{4c}) = 1, \quad u_2(t_{2c}) = u_3(0) = u_3(t_{3c}) = u_4(0) = -1,$$

$$\dot{u}_1(0) = \dot{u}_4(t_{4c}), \quad \dot{u}_1(t_{1c}) = \dot{u}_2(0), \quad \dot{u}_2(t_{2c}) = \dot{u}_3(0), \quad \dot{u}_3(t_{3c}) = \dot{u}_4(0)$$

and includes as unknowns the eight coefficients of the homogeneous solution parts in the four solution segments, the phase φ and the three crossing times t_{1c}, t_{2c} and t_{3c}. The fourth crossing time is determined from the relation $t_{4c} = nT - (t_{1c} + t_{2c} + t_{3c})$. In this case, implementing the solution strategy applied to type II periodic motions and taking advantage of the special form of the solution pieces reduces further the numerical effort to the solution of four equations, involving only t_{1c}, t_{2c}, t_{3c} and φ as unknowns. Numerical solution of this system determines the values of φ and the three crossing times, exploiting the fact that they lie in the intervals $(0, 2\pi)$ and $(0, nT)$ respectively. Finally, the coefficients A_n, B_n $(n = 1\text{–}4)$ and the corresponding periodic motions are evaluated by backsubstitution.

3.4. TYPE IV PERIODIC MOTIONS

In the special cases where the constant component of the forcing term is negligible, the dynamical system examined can exhibit an additional solution type,

namely, the oscillator which may exhibit periodic motions with displacement amplitude confined between -1 and 1. In this case, the equation of motion takes the form

$$\ddot{u} + 2\zeta\dot{u} = \hat{f}_1 \cos(\Omega t + \theta)$$

and accepts an exact solution which has a form identical to (13), but with $A_2 = C_2 = 0$. This means that

$$u(t) = B_2 + D_2 \cos(\Omega t + \theta - \psi),$$

where the amplitude D_2 and the phase ψ are given by equation (14), while the constant B_2 is determined by the initial conditions.

4. STABILITY ANALYSIS

First, it can readily be shown that the *type* IV periodic solutions are always stable, provided that the damping parameter is positive. In addition, the stability properties of *type* I motions can be determined by applying the classical method of linearization [19]. However, the stability analysis for the two remaining types of periodic motions requires the application of a different methodology, due to the abrupt change of parameters occurring at the critical values $u = \pm 1$. The basic ideas of this methodology have been presented in detail in reference [10]. Next, the stability analysis of *type* II motions is presented briefly.

In Figure 3, the solution segments $u_1(t_1)$ and $u_2(t_2)$ represent the two pieces of a type II periodic motion, while the pieces $\bar{u}_1(\bar{t}_1)$ and $\bar{u}_2(\bar{t}_2)$ represent another motion that starts from neighboring initial conditions. First, applying the initial conditions

$$u_1(0) = 1, \quad \dot{u}_1(0) = \dot{u}_{10}$$

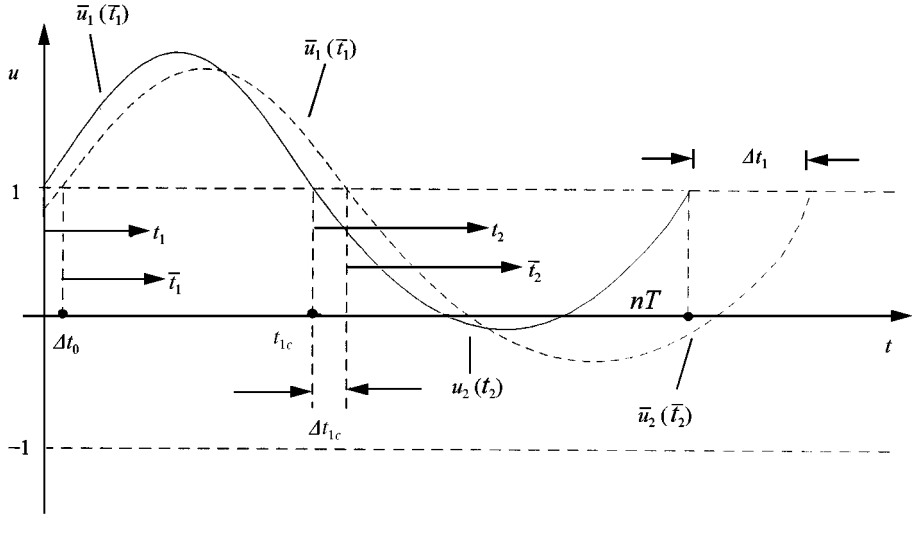

Figure 3. Type II periodic and a neighboring motion.

and employing the solution form (12) leads to a linear system for the unknown coefficients A_1 and B_1. The solution of this system can be expressed in the form

$$A_1 = A_1(\dot{u}_{10}, \varphi), \quad B_1 = B_1(\dot{u}_{10}, \varphi).$$

Next, the solution piece $\bar{u}_1(\bar{t}_1)$, obtained from the initial conditions

$$\bar{u}_1(0) = 1, \quad \dot{\bar{u}}_1(0) = \dot{u}_{10} + \Delta v_0$$

is considered, with $\bar{t}_1 = t_1 - \Delta t_0$. The resulting perturbed solution segment will be given by

$$\bar{u}_1(\bar{t}_1) = A_1(\dot{u}_{10} + \Delta v_0,\ \varphi + \Delta\varphi_0)a_1(\bar{t}_1; \varphi + \Delta\varphi_0) + B_1(\dot{u}_{10} + \Delta v_0, \varphi + \Delta\varphi_0)b_1(\bar{t}_1; \varphi + \Delta\varphi_0) + c_1(\bar{t}_1; \varphi + \Delta\varphi_0)$$

with $\Delta\varphi_0 = \Omega\Delta t_0$. Moreover, this solution satisfies the conditions

$$\bar{u}_1(\bar{t}_{1c}) = 1, \quad \dot{\bar{u}}_1(\bar{t}_{1c}) = \dot{u}_{20} + \Delta v_{1c}, \tag{21}$$

where $\bar{t}_{1c} = t_{1c} + (\Delta t_{1c} - \Delta t_{10})$. Therefore, if the initial perturbations are small, application of conditions (21), followed by appropriate Taylor expansions, leads to a system of two equations, which can be cast in the matrix form

$$\underline{\varepsilon}_{1c} = Q_1 \underline{\varepsilon}_0 \tag{22}$$

after omitting the second and higher order terms. In the last equation, the vectors

$$\underline{\varepsilon}_0 = (\Delta\varphi_0\ \Delta v_0)^{\mathrm{T}}, \quad \underline{\varepsilon}_{1c} = (\Delta\varphi_{1c}\ \Delta v_{1c})^{\mathrm{T}}$$

represent the difference of the perturbed solution from the periodic solution at $t = 0$ and $t = t_{1c}$, respectively, with $\Delta\varphi_{1c} = \Omega\Delta t_{1c}$, while the elements of matrix Q_1 are known functions of the system parameters. Note that the zero order terms drop out from equation (22), because they satisfy conditions (16) and (20).

The difference between the periodic and the perturbed solution in the second interval of the motion is obtained in a similar manner. In this case, application of the initial conditions

$$u_2(0) = 1, \quad \dot{u}_2(0) = \dot{u}_{20}$$

determines first the coefficients A_2 and B_2. Then, the perturbed solution piece $\bar{u}_2(\bar{t}_2)$, obtained from the neighboring starting conditions

$$\bar{u}_2(0) = 1, \quad \dot{\bar{u}}_2(0) = \dot{u}_{20} + \Delta v_{1c}$$

with $\bar{t}_2 = t_2 - \Delta t_{1c}$, must satisfy the conditions

$$\bar{u}_2(\bar{t}_{2c}) = 1, \quad \dot{\bar{u}}_2(\bar{t}_{2c}) = \dot{u}_{10} + \Delta v_{2c} \tag{23}$$

with $\bar{t}_{2c} = t_{2c} + (\Delta t_{2c} - \Delta t_{1c})$. Application of conditions (23) yields two equations, which after neglecting second and higher order terms can be put in the form

$$\underline{\varepsilon}_1 = Q_2\, \underline{\varepsilon}_{1c}, \tag{24}$$

where the vector $\underline{\varepsilon}_1 = (\Delta\varphi_1\ \Delta v_1)^{\mathrm{T}}$ includes the difference between the perturbed and the periodic solution at time $t_2 = t_{2c}$ and $\Delta\varphi_1 = \Omega\,\Delta t_{2c}$. Again, the zero order terms

cancel out, because they satisfy conditions (18) and (19). Therefore, combination of equations (22) and (24) yields

$$\underline{\varepsilon}_1 = Q\underline{\varepsilon}_0, \tag{25}$$

where $Q \equiv Q_2 Q_1$. The last matrix relation determines the error at the end of the first response period when the original error in the initial conditions is known. Therefore, after neglecting the higher order terms, the original error disappears gradually provided that all the eigenvalues of the matrix Q have modulus less than one [14]. In such cases, the periodic solution examined is stable. If at least one eigenvalue of matrix Q has modulus larger than one, the original error grows with time and the periodic solution is unstable. On the other hand, when at least one eigenvalue of Q has modulus equal to one, while the other eigenvalue has modulus smaller than one, the corresponding periodic solution exhibits a bifurcation [12].

Finally, the stability analysis of *type* III periodic motions is very similar to that presented for type II motions. The main difference is due to the fact that these motions consist of four discrete segments. As a consequence, application of the same methodology over a response period leads to a relation identical to equation (25), where the new matrix Q is now a product of four matrices, instead.

5. SOME SIMPLER GEAR-PAIR MODELS

Depending on the accuracy level required in the results, several approximations of the original gear-pair equation of motion are considered in practice. These cases are analyzed and presented separately in the remainder of this section.

5.1. LINEAR MODELS

In the simplest approximation, both the gear backlash and mesh stiffness variation is neglected [3]. This means that

$$g(u) = u, \quad w(t) = 1$$

and the gear-pair dynamics is governed by the following linear time-invariant equation of motion

$$\ddot{u} + 2\zeta\dot{u} + u = f_0 + \hat{f}_1 \cos(\Omega t + \theta).$$

In such cases, the equivalent constant stiffness of the model coincides with the mean stiffness of the gear-pair and the exact solution can be obtained in closed form. Including the mesh stiffness variation but neglecting backlash, that is for

$$g(u) = u \quad \text{and} \quad w(t) = 1 + 2\varepsilon \cos \Omega t,$$

leads to a better approximation, expressed by the following linear time-variant equation of motion:

$$\ddot{u} + 2\zeta\dot{u} + (1 + 2\varepsilon \cos \Omega t)u = f_0 + \hat{f}_1 \cos(\Omega t + \theta).$$

The solution and stability procedure for the last equation is similar to that presented for the type I periodic motions and is therefore not repeated here.

5.2. NON-LINEAR MODEL

Another approximate model of the gear-pair response can be obtained by considering the mesh stiffness variation and modelling the gear clearance with a weakly non-linear symmetric spring. In this case, equation (4) becomes

$$\ddot{u} + 2\varepsilon\mu\dot{u} + (1 + 2\varepsilon\cos\Omega t)(u + \varepsilon\alpha u^3) = f_0 + \varepsilon f_1\cos(\Omega t + \theta), \tag{26}$$

representing the equation of motion of a Mathieu–Duffing oscillator under the simultaneous action of parametric and external forcing. Applying standard perturbation procedures [19], the approximate solution of the last equation within the frequency range specified by condition (3) is obtained in the form

$$u(t) = f_0 + a\cos(\Omega t - \gamma) + O(\varepsilon),$$

with amplitude and phase of the oscillatory term satisfying the following set of slow-flow equations:

$$a' = -\mu a - f_0\sin\gamma + \tfrac{1}{2}f_1\sin(\gamma + \theta),$$

$$a\gamma' = (\sigma - \tfrac{3}{2}\alpha f_0^2)a - \tfrac{3}{8}\alpha a^3 - f_0\cos\gamma + \tfrac{1}{2}f_1\cos(\gamma + \theta).$$

Obviously, constant solutions of these equations correspond to periodic motions of the gear-pair system, with fundamental frequency Ω. Such solutions can be determined by solving a system of algebraic equations in the form

$$\hat{e}_1\sin\gamma + \hat{e}_2\cos\gamma = \hat{e}_3 a, \quad \hat{e}_4\sin\gamma + \hat{e}_5\cos\gamma = \hat{e}_6 a + \hat{e}_7 a^3. \tag{27}$$

The solution process for the last system starts by first solving it for $\sin\gamma$ and $\cos\gamma$. Squaring and adding the resulting expressions eliminates the phase γ and leads to a cubic polynomial in a^2, which can be solved in closed form for the vibration amplitude a. Then, the corresponding phase γ is determined by a simple substitution. Finally, the stability properties of these solutions can be obtained by applying the classical method of linearization [19].

5.3. PIECEWISE LINEAR MODEL

As a final special case, the gear-pair response may be obtained by employing the following approximate piecewise linear equation of motion:

$$\ddot{u} + 2\zeta\dot{u} + g(u) = f_0 + \hat{f}_1\cos(\Omega t + \theta + \varphi). \tag{28}$$

This equation is obtained by neglecting the gear mesh stiffness variation, i.e., by setting $w(t) = 1$ in equation (3), but including the backlash. Equation (28) accepts all four periodic solution types of equation (3). However, the determination of these motions becomes much easier in the present case.

In particular, *type* I and *type* IV periodic motions are governed by linear equations of motion with constant coefficients and can be obtained in closed form. Likewise, *type* II periodic motions are determined by imposing the set of matching and periodicity conditions (15)–(20), but their evaluation is easier since the exact solution form can now be obtained even in the first time interval $0 \leqslant t_1 \leqslant t_{1c}$. More specifically, by employing a methodology similar to that presented in reference [14], the displacement conditions (15)–(18) are first applied and yield the following expressions for the coefficients of the homogeneous solutions within the two discrete time intervals of a periodic type II motion

$$A_m = A_{m0} + A_{ms}\sin\varphi + A_{mc}\cos\varphi, \quad B_m = B_{m0} + B_{ms}\sin\varphi + B_{mc}\cos\varphi \quad (m = 1, 2).$$

The coefficients on the right-hand side of these expressions are known functions of the system parameters and the crossing time t_{1c}. Then, application of the velocity conditions (19) and (20) leads to two algebraic equations of the form

$$E_{ms}\sin\varphi + E_{mc}\cos\varphi = E_{m0} \quad (m = 1, 2).$$

Elimination of the $\sin\varphi$ and $\cos\varphi$ terms from the last two equations yields a single transcendental equation, whose numerical solution furnishes t_{1c}. Eventually, the rest of the unknowns are evaluated by simple backsubstitutions (see reference [14]).

A similar methodology is applied for *type* III periodic motions of equation (28). These motions are obtained by imposing a set of matching and periodicity conditions, which is identical to that imposed on equation (3), but their determination is easier since the exact solution form can be obtained in all four time intervals of these solutions. Employing a methodology similar to that presented above for type II motions and in reference [15], the determination of these motions is reduced to the solution of three transcendental equations for the three crossing times t_{1c}, t_{2c} and t_{3c}. Finally, the stability analysis for all the periodic solutions of equation (28) is performed by applying the same procedures employed for the corresponding solution types of equation (3).

6. NUMERICAL RESULTS

The analysis presented in the previous sections is applied to several gear-pair systems, in an effort to demonstrate its effectiveness and accuracy as well as to capture phenomena related to the gear-pair dynamics. For small values of the parameter ε, the results obtained are first compared with the results of previous related studies [6–10, 14, 15] and with direct integration. Apart from ε, representing the amplitude of the meshing stiffness variation, the other technical parameters consist of the damping parameter ζ, the forcing amplitudes f_0 and f_1, the phase θ and the forcing frequency. The effects of these parameters on the existence and stability properties of periodic motions of gear-pair systems are investigated by presenting series of response diagrams. In all these diagrams, branches of periodic stable/unstable solutions are represented by solid/dashed curves, respectively.

In the first sequence of response diagrams, Figure 4 presents results obtained for a system with parameters: $\varepsilon = 0{\cdot}03$, $\mu = 0{\cdot}8$, $\theta = 0, f_1 = 2{\cdot}5$ and five different values of the constant forcing parameter f_0. For relatively large values of f_0, only type I

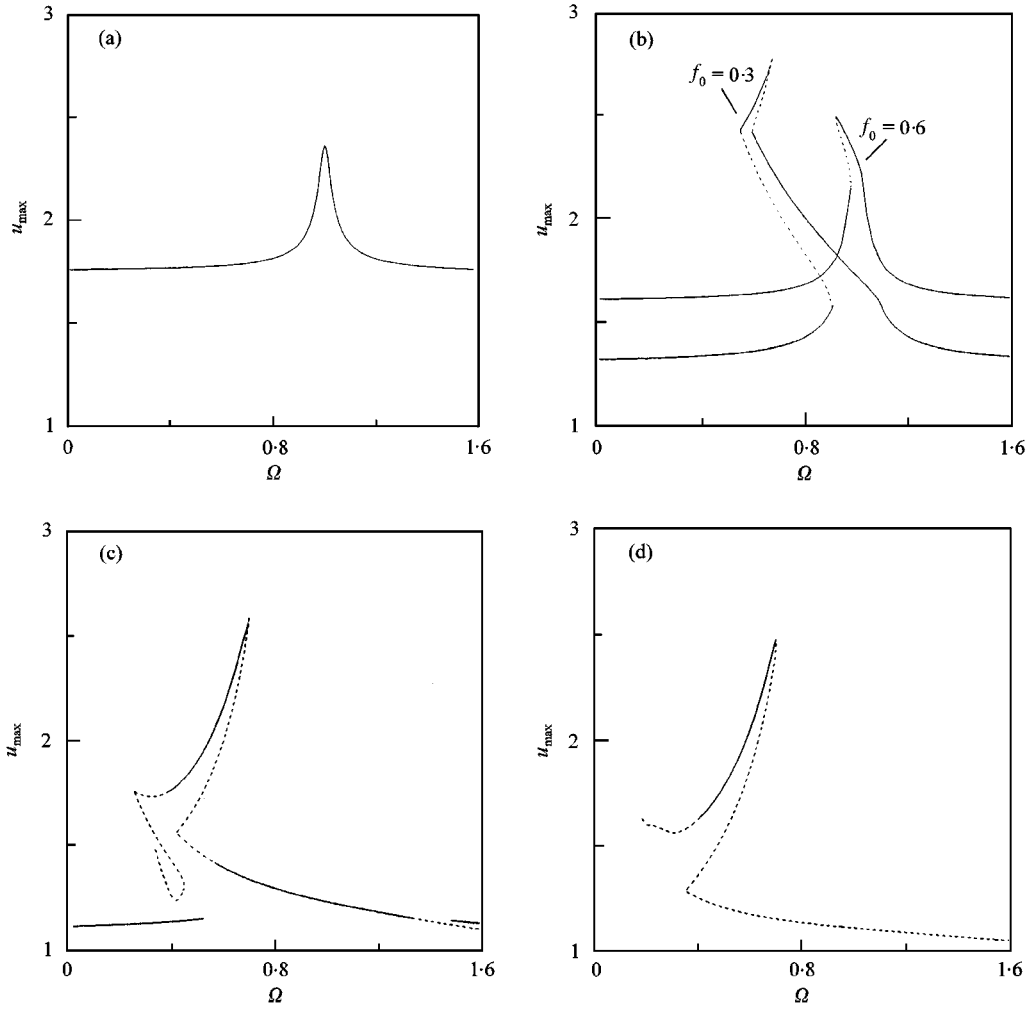

Figure 4. Effect of constant forcing parameter ($\varepsilon = 0{\cdot}03$, $\zeta = 0{\cdot}024$, $f_1 = 2{\cdot}5$, $\theta = 0$): (a) $f_0 = 0{\cdot}75$; (b) $f_0 = 0{\cdot}6$ and $0{\cdot}3$; (c) $f_0 = 0{\cdot}075$; (d) $f_0 = 0{\cdot}03$.

periodic motions, involving no gear-teeth impacts, are possible. Moreover, for this type of motions, the resonance occurs in the vicinity of $\Omega = 1$, since the system is essentially linear (Figure 4(a)). As the value of f_0 decreases, the type I motions withdraw gradually, giving way to type II and III motions, which involve single and double-sided impacts respectively. Among them, the type II solution branches exhibit softening behavior, while the type III branches present hardening behavior, just like that observed for similar piecewise linear oscillators with constant coefficients [14]. As a result of the bending in the solution branches, multiple stable solutions may coexist, making possible the appearance of classical jump phenomena. Note that similar response aspects were also investigated in references [6–8], by employing direct integration, harmonic balance and shooting methods.

The frequency range shown in the response diagrams of Figure 4 is much greater than that covered by the resonance condition (3). However, it is necessary to

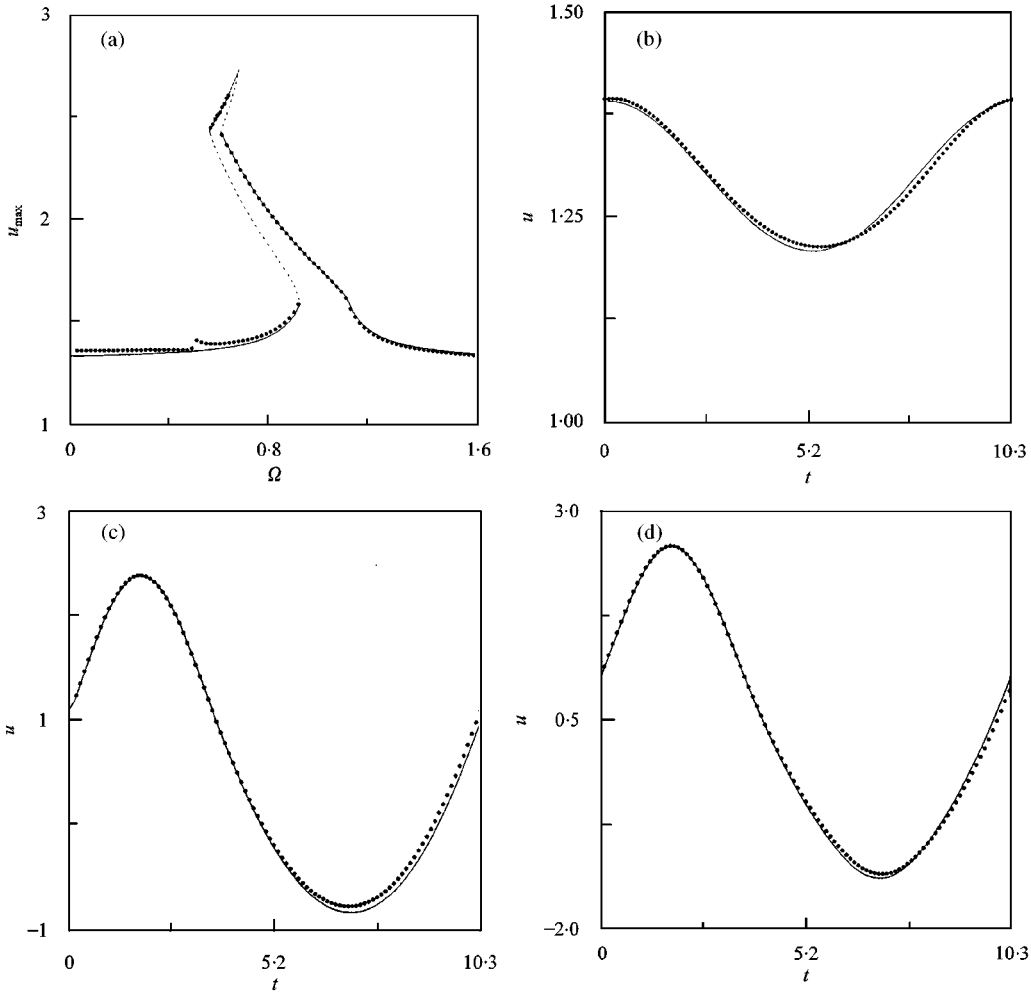

Figure 5. Comparison of results obtained by the analytical method with results obtained by direct integration (represented by dots): (a) response diagram for $f_0 = 0{\cdot}03$; (b) type I motion; (c) type II motion; (d) type III motion.

consider this greater frequency range due to the large bending of the solution branches induced by the strong backlash non-linearity within the range of the examined resonance. Next, in order to check the accuracy, effectiveness and validity of the analysis employed in the present study. Figure 5 compares the results obtained for the case with $f_0 = 0{\cdot}3$ with results obtained for the same set of parameters by direct integration of the original equation of motion (4). This forcing value was chosen because it gives rise to type I, II and III motions. First, Figure 5(a) compares results on the response diagram. Clearly, the agreement between the analytical and the numerical results (represented by dots) in the frequency range expressed by equation (3) is quite good. In addition, Figures 5(c) and (d) compare response histories of type I, II and III motions, obtained at $\omega = 0{\cdot}61$ by the present method (continuous line) and by direct integration (dots). Again, the agreement is good and indicates the validity of the new method.

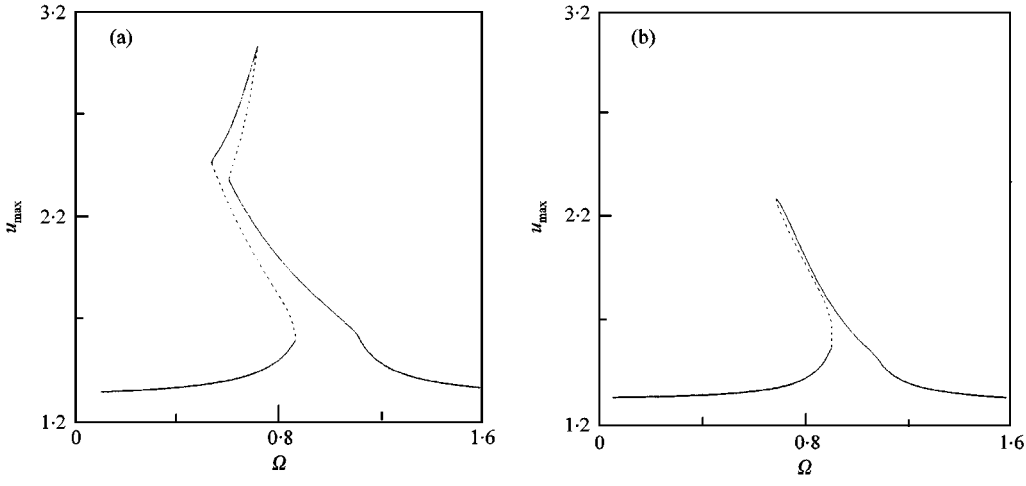

Figure 6. Effect of stiffness variation parameter: (a) $\varepsilon = 0{\cdot}001$; (b) $\varepsilon = 0{\cdot}2$.

The effect of the stiffness variation parameter is shown in Figure 6, For these response diagrams, the parameters are chosen so that the values of ζ, θ and $\hat{f}_1$ remain the same as in the first example, while the value of f_0 is held fixed at 0·3. A direct conclusion is that an increase in the value of ε causes a gradual elimination of type III motions and a reduction in the maximum response amplitude, in the case examined. Moreover, note that the response diagram in Figure 4(b) corresponding to $f_0 = 0{\cdot}3$ is part of the same sequence. Therefore, comparison of this figure with Figure 6(a) shows that the influence of the stiffness time variation on the response weakens for relatively small values of ε, as expected.

Simple inspection of the response diagrams shown in Figures 4 and 6 reveals that the commonly employed linear gear-pair models presented in section 5 will fail to capture the essential dynamic behavior of the gear-pair system in most of the cases. Likewise, the non-linear model with equation of motion (26) will also provide poor results in most instances, because the solutions of system (27) yield response like the classical Duffing oscillator. On the other hand, the piecewise linear model presented in section 5 may yield sufficiently accurate results in some cases, as explained next.

Figure 7(a) has been obtained for the set of parameters that led to the response diagrams of Figure 6 and $\varepsilon = 0$ (i.e., for $\zeta = 0{\cdot}024$, $f_0 = 0{\cdot}3$, $\hat{f}_1 = 0{\cdot}075$, $\theta = 0$), by solving the equation of motion (28) instead of equation (4). Comparison with Figure 6(a) reveals that the results obtained for the model presented at the end of section 5, which ignores the mesh stiffness periodic variations, become quite accurate for relatively small values of ε. Next, Figure 7(b) is obtained by increasing the value of $\hat{f}_1$ to 0·4. A simple comparison with Figure 7(a) confirms that apart from an increase in the motion amplitudes, an increase in $\hat{f}_1$ brings a gradual withdrawal of type I motions – especially those lying originally in the low-frequency range – and a domination of type III and II motions. Also, at some frequency value, the type II periodic motions lose stability through a period-doubling bifurcation. As a result, $n = 2$ subharmonic motions appear in that frequency range, which are captured and shown in Figure 7(b).

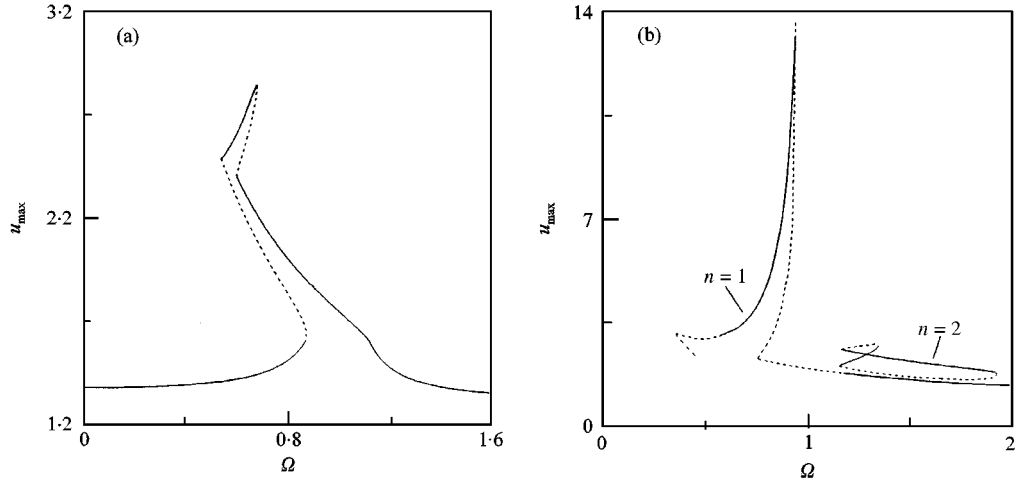

Figure 7. Effect of forcing parameter $\hat{f}_1$: (a) $\hat{f}_1 = 0{\cdot}075$; (b) $\hat{f}_1 = 0{\cdot}4$.

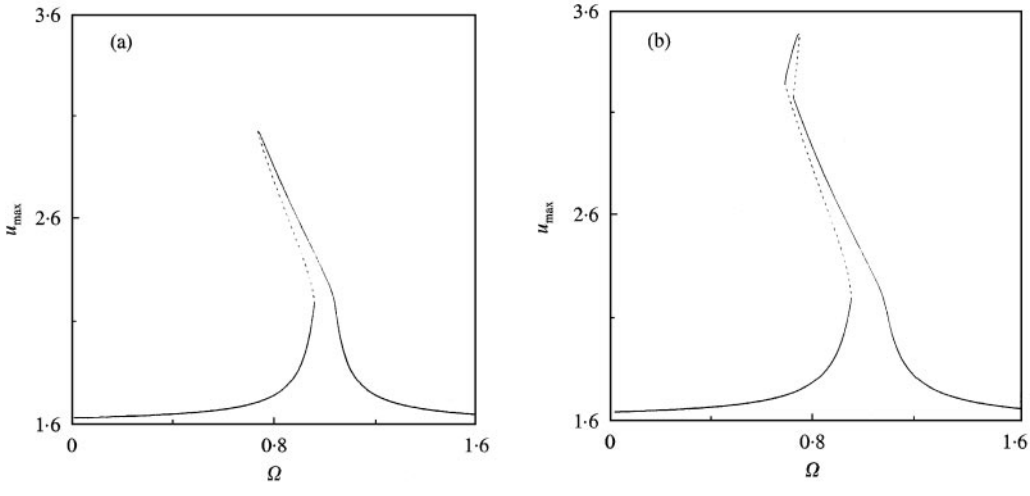

Figure 8. Effect of forcing phase parameter: (a) $\theta = \pi/4$; (b) $\theta = \pi/2$.

Next, Figure 8 shows response diagrams obtained for $\varepsilon = 0{\cdot}1$, $\mu = 0{\cdot}5$, $f_0 = 0{\cdot}5$, $f_1 = 2$ and two different values of θ. These results demonstrate the effect of the phase θ of the harmonic forcing term in the response. For the set of parameters chosen, a change in the strength of the out-of-phase forcing component, represented by θ, is shown to have an important influence on the form of the response diagrams.

In the final part of the parametric study, the effect of the damping parameter on the system periodic response is investigated. Figure 9(a) is obtained for the same set of parameters as that of the first example, with $f_0 = 0$, while for the response diagram of Figure 9(b) the damping parameter value is reduced to $\mu = 0{\cdot}1$. Clearly, the larger the value of the damping parameter, the smaller the solution amplitude, as expected.

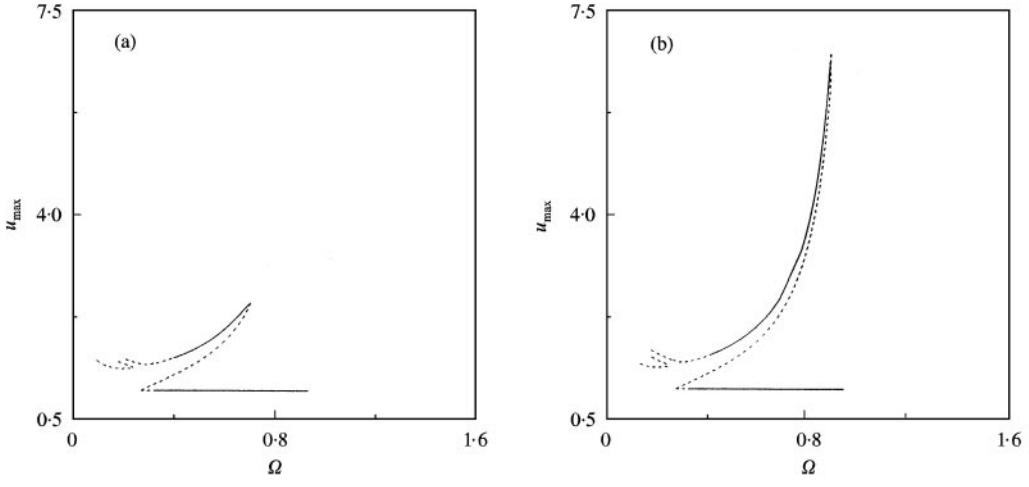

Figure 9. Effect of damping parameter: (a) $\mu = 0{\cdot}8$; (b) $\mu = 0{\cdot}1$.

Apart from periodic motions, the oscillator examined can exhibit more complicated and rich dynamic response. This was demonstrated by performing direct integration of the original equation of motion in frequency ranges where no stable periodic solutions are captured. For instance, Figure 10 shows a typical sequence of response histories, obtained for the combination of parameters that led to the response diagram of Figure 9(b). First, a period-doubling cascade was detected. Namely, the $n = 1$ periodic solution obtained at $\Omega = 0{\cdot}226$ (Figure 10(a)) is replaced by an $n = 2$ (Figure 10(b)) and then by an $n = 4$ (Figure 10(c)) subharmonic motion, by gradually decreasing the value of the forcing frequency Ω. At about $\Omega = 0{\cdot}221314$, this motion undergoes a boundary crisis and exhibits apparently chaotic response [12, 20]. In fact, in a specific frequency interval, the response presents intermittent chaos, in accordance with previously reported experimental results [9]. More specifically, immediately below the frequency interval where the $n = 4$ motion is stable, the response is found to switch temporarily between intervals of regular motion—resembling the previously existing $n = 4$ motion—and chaotic response, as illustrated by the response histories shown in Figures 10(d) and (e) (Figure 11 presents the corresponding Poincare sections during intervals of regular and irregular response respectively). The intervals of the chaotic motion are small at the beginning—relative to the intervals of the regular response—and increase gradually, by decreasing the value of Ω, up until about $\Omega = 0{\cdot}2203$, where the motion becomes completely chaotic. Eventually, at some smaller value of Ω, the chaotic response settles to an $n = 1$ harmonic motion, through another boundary crisis. Again, by decreasing the value of Ω below the crisis value, the transition from chaotic to periodic response is completed in a progressively shorter time [20].

The numerical results presented so far exhibit many similarities with results obtained in previous analytical studies on piecewise linear systems [13–15] and especially with numerical and experimental results on gear systems [6–10]. In particular, the validity of the mechanical model employed has been checked in

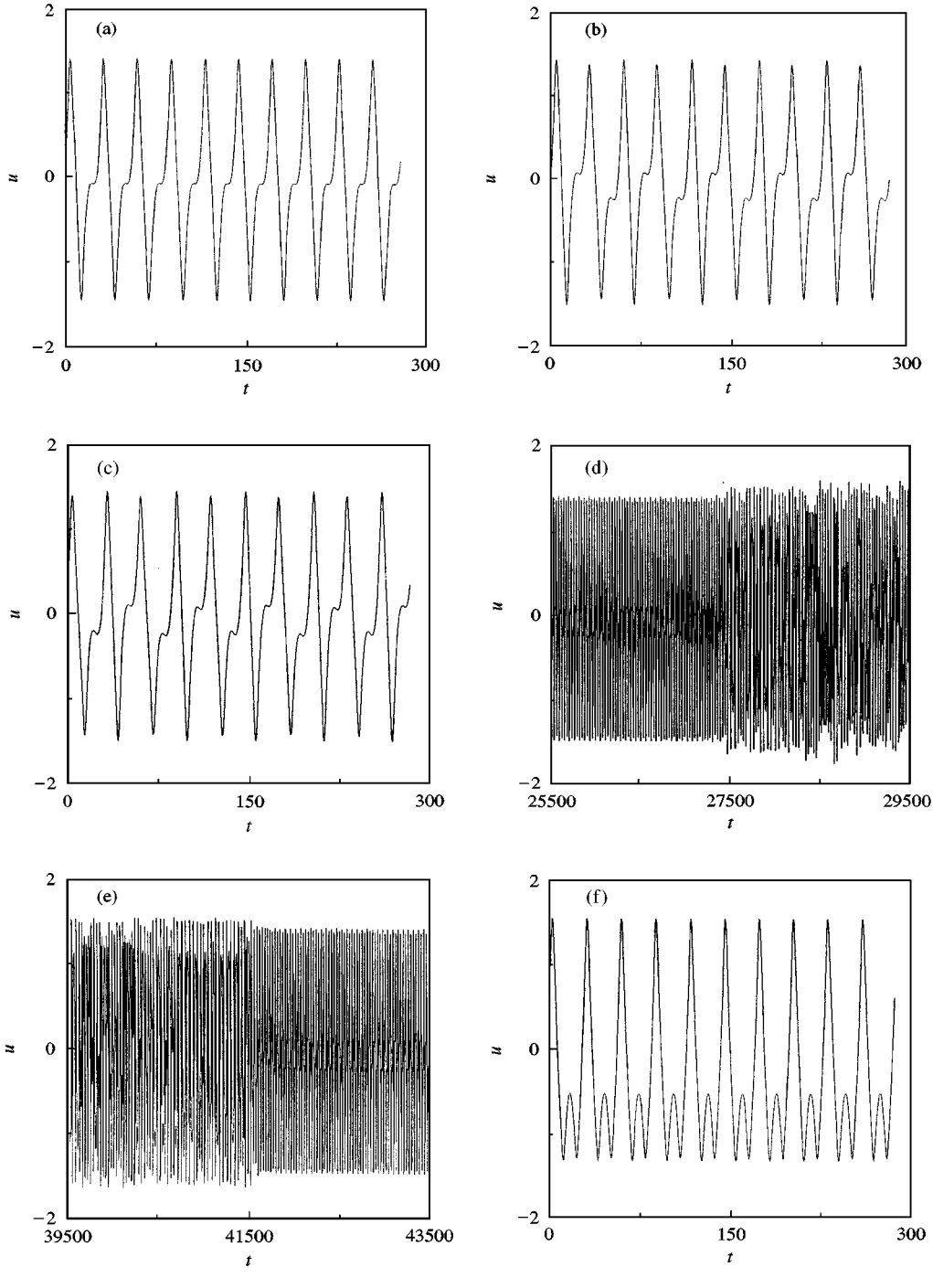

Figure 10. Response histories at: (a) $\Omega = 0{\cdot}226$; (b) $\Omega = 0{\cdot}22195$; (c) $\Omega = 0{\cdot}2215$; (d) and (e) $\Omega = 0{\cdot}221314$; (f) $\Omega = 0{\cdot}2203$.

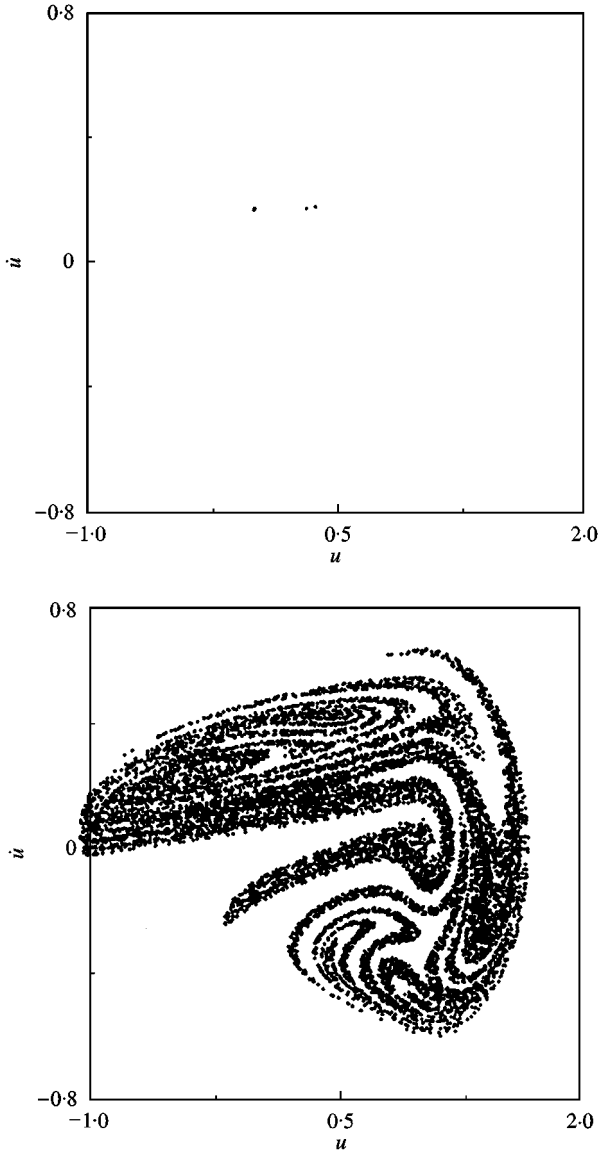

Figure 11. Poincare sections $(u, \dot{u})$ at $\Omega = 0{\cdot}221314$ during intervals of regular and irregular response.

earlier studies (see e.g., references [6, 7]), where comparisons between numerical results with available experimental data indicated good agreement. Moreover, the results of the present study exhibit many qualitative characteristics similar to those of a recent experimental study on the same mechanical model [9].

Finally, numerical integration is also employed in order to demonstrate the validity of the present analysis even when higher harmonics are included in the gear-pair equation of motion for the gear mesh stiffness and the external excitation. For this purpose, the first example system with $f_0 = 0{\cdot}3$ is re-examined. More specifically, Figure 12 shows a comparison between the results obtained by the

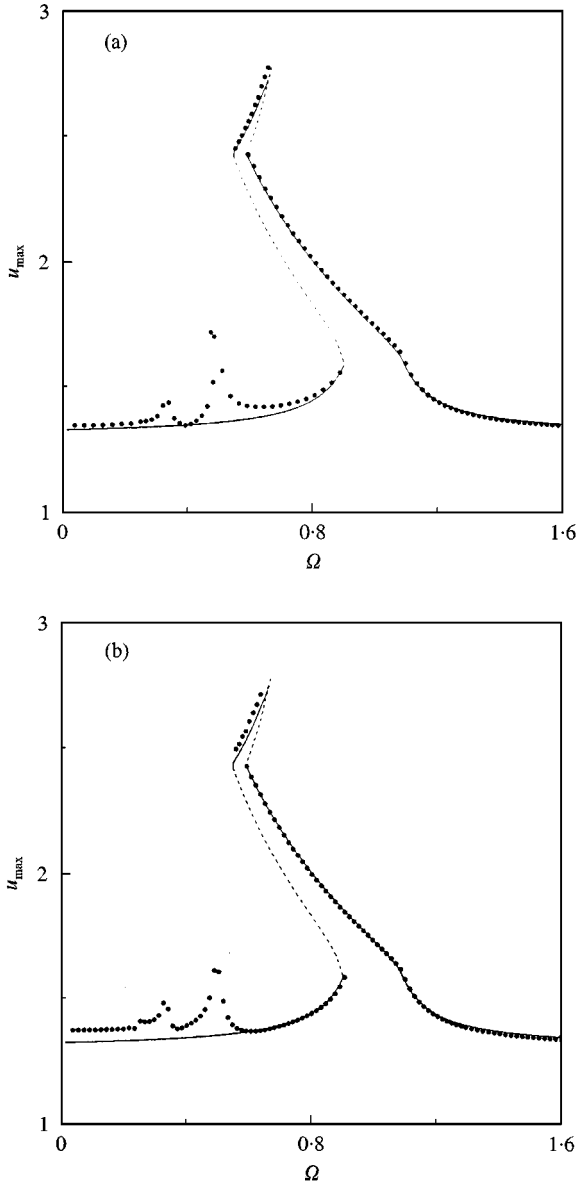

Figure 12. Comparison of results obtained by the new analytical method with results obtained by direct integration of equation (2): (a) system with periodic stiffness variation only; (b) system with periodic stiffness variation and periodic external forcing.

present analysis with results obtained by direct integration of the equation of motion (2). Initially, Figure 12(a) presents results for a case with

$$w(t) = 1 + 2\sum_{n=1}^{3} \varepsilon_n \cos(n\Omega t), \quad f(t) = f_0 + \varepsilon f_1 \cos(\Omega t + \theta)$$

and $\varepsilon_1 = \varepsilon = 0{\cdot}03$, $\varepsilon_2 = 0{\cdot}02$, $\varepsilon_3 = 0{\cdot}01$. Obviously, the results obtained by direct integration (represented by dots) demonstrate the existence of superharmonic

resonances in the low forcing frequency range, as expected [6–8, 19]. However, even in this case, the results show good agreement in the range of the resonance expressed by condition (3). Similar conclusions are drawn from the results of Figure 12(b), where the direct integration was conducted for a more complex system with

$$w(t) = 1 + 2\sum_{n=1}^{3} \varepsilon_n \cos(n\Omega t), \quad f(t) = f_0 + \varepsilon \sum_{n=1}^{3} f_n \cos(n\Omega t + \theta)$$

and $f_1 = 2{\cdot}5$, $f_2 = 1$, $f_3 = 0{\cdot}5$. Again, the main discrepancy is limited to the low forcing frequency range, while the agreement in the resonance range examined is satisfactory.

7. SUMMARY

In the first part of the present study, analytical methods were employed for determining periodic steady state response of gear-pair systems. Initially, the equation of motion was set up in a general form, for gear systems including backlash and time-dependent stiffness. Then, by assuming periodic external forcing and meshing stiffness variations, several possible types of periodic response were identified and determined by employing approximate analytical methodologies, for conditions of simultaneous fundamental parametric resonance and principal external resonance. These methods combine approaches which are applicable to dynamical systems with piecewise linear characteristics and to oscillators involving time-dependent coefficients. In addition, for all cases examined, suitable methodologies were also developed, determining the stability properties of the located periodic motions. In particular, for models with non-zero backlash, the stability analysis was performed by first determining the propagation of small errors in the initial conditions over a response period. The analytical part was completed by investigating the response and stability of some simpler but practically important gear-pair models.

In the second part of the study, numerical results were presented for several examples of gear-pair models. First, series of response diagrams were obtained, illustrating the effect of all the technical parameters on the response. More specifically, it was shown that for relatively large values of the constant external forcing parameter, only periodic motions involving no impacts are possible and the system is essentially linear. However, for smaller values of this parameter, motions involving single- and double-sided impacts become possible. Likewise, the influence of the gear meshing stiffness variation parameter on the response was shown to weaken for small values of this parameter. As far as the phase in the harmonic forcing term is concerned, it was shown to influence both the type and the amplitude of the periodic response. In the final series of the response diagrams, the effect of the damping parameter on the system periodic response was investigated and it was verified that an increase in its value causes a decrease in the amplitude of the solution. Based on these results, it was shown that the simpler gear-pair models, which are employed frequently in practice, may not be suitable to capture their real dynamics. The study concluded by demonstrating that apart from the classical

jump phenomena and period-doubling cascades, the gear-pair system can exhibit more complicated dynamic response, in accordance with the behavior observed in previous experimental studies. In particular, by performing direct integration of the original equation of motion, a sequence of response histories was presented, accompanied by Poincare sections, demonstrating the occurrence of boundary crises and intermittent chaos.

REFERENCES

1. R. W. Gregory, S. L. Harris and R. G. Munro 1963 *Proceedings of the Institution of Mechanical Engineers* **178**, 1–28. Dynamic behavior of spur gears.
2. J. W. Lund 1978 *ASME Journal of Mechanical Design* **100**, 535–539. Critical speeds, stability and response of a geared train of rotors.
3. H. N. Ozguven and D. R. Houser 1988 *Journal of Sound and Vibration* **121**, 383–411. Mathematical models used in gear dynamics—a review.
4. C. -S. Chen 1993 *Ph. D. Dissertation, Arizona State University*. Coupled lateral-torsional vibrations of geared rotor-bearing systems.
5. C. -S. Chen, S. Natsiavas and H. D. Nelson 1997 *ASME Journal of Vibration and Acoustics* **119**, 85–88. Stability analysis and complex dynamics of a gear-pair system supported by a squeeze film damper.
6. A. Kahraman and R. Singh 1991 *Journal of Sound and Vibration* **146**, 135–156. Interactions between time-varying mesh stiffness and clearance nonlinearities in a geared system.
7. C. Padmanabhan and R. Singh 1996 *Journal of the Acoustical Society of America* **99**, 324–334. Analysis of periodically forced nonlinear Hill's oscillator with application to a geared system.
8. A. Kahraman and G. W. Blankenship 1996 *Journal of Sound and Vibration* **194**, 317–336. Interactions between commensurate parametric and forcing excitations in a system with clearance.
9. A. Kahraman and G. W. Blankenship 1997 *Journal of Applied Mechanics* **64**, 217–226. Experiments on nonlinear dynamic behavior of an oscillator with clearance and periodically time-varying parameters.
10. S. Natsiavas, S. Theodossiades and I. Goudas 1999. *International Journal of Nonlinear Mechanics*. Dynamic analysis of peicewise linear oscillators with time periodic coefficients. (accepted).
11. F. F. Ehrich (editor) 1992 *Handbook of Rotordynamics*. New York: McGraw-Hill.
12. A. H. Nayfeh and B. Balachandran 1995 *Applied Nonlinear Dynamics*. New York: John Wiley & Sons.
13. S. W. Shaw and R. H. Rand 1989 *International Journal of Nonlinear Mechanics* **24**, 41–56. The transition to chaos in a simple mechanical system.
14. S. Natsiavas 1990 *International Journal of Nonlinear Mechanics* **25**, 535–554. On the dynamics of oscillators with bilinear damping and stiffness.
15. S. Natsiavas and H. Gonzalez 1992 *Journal of Applied Mechanics* **59**, S284–S290. Vibration of harmonically excited oscillators with asymmetric constraints.
16. R. J. Comparin and R. Singh 1989 *Journal of Sound and Vibration* **134**, 259–290. Non-linear frequency response characteristics of an impact pair.
17. F. Peterka and T. Kotera 1996 *Machine Vibration* **71**, 71–82. Four ways from periodic to chaotic motion in the impact oscillator.
18. S. Foale and S. R. Bishop 1992 *Philosophical Transactions of the Royal Society of London* **A338**, 547–556. Dynamical complexities of forced impacting systems.
19. A. H. Nayfeh and D. T. Mook 1979 *Nonlinear Oscillations*. New York: Wiley–Interscience.
20. A. K. Bajaj 1991 *International Series of Numerical Mathematics* **97**, 27–36. Examples of boundary crisis phenomenon in Structural Dynamics.